Performance of Signal Detection Scheme Based on Lattice Reduction in Spatial Multiplexing UWB Systems

Youngbeom Kim and Sangchoon Kim
Department of Electronics Engineering, Dong-A University, Busan, Korea
Email: kiyoubeo@donga.ac.kr; sckim@dau.ac.kr

***Abstract*—This paper proposes a Lattice-Reduction (LR)-aided Zero-Forcing (ZF) detection method for spatial multiplexing Ultra-Wideband (UWB) Multiple Input Multiple Output (MIMO) systems on indoor log-normal multipath fading channels. It is analytically shown that it can obtain the maximum achievable diversity gain, which is the product of the number of resolvable multipath components and the number of receive antennas. The analytical BER performance is compared with the simulated results. It is also seen through simulations and theoretical results that the LR-based ZF signal detection scheme outperforms the other receivers using ZF detector without LR.**

***Index Terms*—Lattice Reduction (LR), log-normal fading, Multiple Input Multiple Output (MIMO), spatial multiplexing, Ultra-Wideband (UWB)**

I. Introduction

Ultra-Wideband (UWB) communications have been considered as a promising technology for use in very high data rate wireless personal-area networks [1], [2] and Wireless Sensor Networks (WSN) [3]. Spatial Multiplexing (SM) Multiple Input Multiple Output (MIMO) techniques [4] can be applied to UWB systems as one solution to the increasing demand of various indoor wireless applications for higher-rate reliable communications [5], [6]. In [7], noncoherent MIMO UWB systems have been examined on a basis of differential space-time block code. In [8], the performance of UWB-MIMO systems for wireless body area networks has been evaluated using spreading code and Maximum-Likelihood (ML) detection. In [9] and [10], UWB systems for WSN have been combined with multiple antennas. In [11], the error rate performance of a multi-antenna Rake receiver has been analyzed over UWB indoor lognormal multipath fading channels. In order to separate the spatially multiplexed data, the detector has performed zero-forcing and maximum ratio combining (called a ZF-MRC). When UWB MIMO systems with N_T transmit antennas, N_R receive antennas, and L resolvable multipath components are employed, the diversity order of the ZF-MRC receiver is given by $L(N_R - N_T + 1)$. To enhance the diversity gain of the UWB MIMO detector, the other detection architecture has been proposed in [12]. At first, the receiver has carried out maximum ratio combining for each path component and then multipath combining. Both combining actions correspond to 2-dimensional Rake operation in space and time domain. Next, a zero-forcing scheme is used to spatially demultiplex the incoming data stream. This detection method is called an MRC-ZF. It has been shown to achieve the improved diversity gain of $LN_R - N_T + 1$. However, it cannot obtain the maximum diversity gain of LN_R because the performance of ZF receiver is suboptimal.

In [13] and [14], Lattice Reduction (LR) equalization [15], [16] under zero-padded block transmission has been employed in Rayleigh faded frequency-selective MIMO channels. It has been analytically shown in [14] that a two-stage LR-aided decoder can obtain the full diversity gain of LN_R, which is the same as that of ML detector. If LR techniques are adopted for SM UWB MIMO detection based on the 2-dimensional Rake scheme, the largest diversity gain could be achieved. In this paper, we propose an LR-assisted signal detection scheme with a single ZF filter over indoor log-normal multipath fading channels. It is known that the performance of the ZF receiving filter is similar that of the Minimum Mean Square Error (MMSE) receiver at high Signal-to-Nose Ratios (SNRs). This paper considers only the ZF associated receiving architecture. The MRC-ZF scheme is extended to the LR domain. It is also shown that the proposed LR-based ZF detector offers the same maximum diversity order as that of the ML receiver, which is equal to LN_R. Thus the diversity gain of the LR-based ZF detector is larger than that of the MRC-ZF. We analytically examine the theoretical Bit Error Rate (BER) performance of the LR-based signal detection scheme in a SM UWB MIMO receiver. Furthermore, it is seen that it has better BER performances than those of the MRC-ZF and ZF-MRC receivers. Finally, simple complexity comparison of all receiving schemes is presented.

II. System Model

Consider a pulsed SM UWB MIMO system composed by N_T transmit antennas and N_R receive antennas, where

Manuscript received September 27, 2018; revised December 25, 2018; accepted December 25, 2018.

Corresponding author: Sangchoon Kim (email: sckim@dau.ac.kr).

doi: 10.18178/ijeetc.8.4.205-212

the transmitted data streams are demultiplexed over the N_T transmit antennas. Assuming that the binary pulse-amplitude modulation (2PAM) scheme is employed, the UWB signal transmitted from the nth transmit antenna is expressed as

$$s_n(t) = \sum_{k=-\infty}^{\infty} \sqrt{E_b}\, b_n(k) p(t - kT_b) \tag{1}$$

where E_b is the average bit energy, $b_n(k)$ is the kth information bit from the nth transmit antenna, $p(t)$ is the unit energy UWB pulse of short duration, and T_b is the bit interval (much larger than the pulse duration).

Among UWB wireless multipath channel models examined in the literature, a dense multipath channel could be observed in indoor office and industrial environments [17], [18]. In this model, each resolvable delay bin contains significant energy and resolvable multipath components have regularly spaced arrival times. It has been called a tapped-delay-line (TDL) multipath model, which has been used in [11] to approximate the exact channel model. Adopting the TDL model in this paper, the channel impulse response can be described as [11], [17]

$$c_{mn}(t) = \sum_{t=0}^{L_t - 1} h_{mn}(l) \delta(t - lT_p) \tag{2}$$

where L_t is the total number of resolvable multipaths, $\delta(t)$ is the Dirac delta function, T_p is the minimum multipath resolution, which is equal to the width of the pulse $p(t)$, and $h_{mn}(l)$ is the channel fading coefficient of the lth resolvable path for the signal to the mth receive antenna transmitted from the nth transmit antenna whose amplitude has a log-normal distribution. The channel gain $h_{mn}(l)$ can be given by $h_{mn}(l) = \zeta_{mn}(l) g_{mn}(l)$, where the random variable $\zeta_{mn}(l)$ takes +1 and −1 with equal-likelihood to account for pulse-phase inversion and the variable $g_{mn}(l)$ is the fading magnitude term to obey a log-normal distribution.

After propagating through the frequency-selective multipath channel depicted by (2), the transmitted signals from all N_T transmit antennas arrive at the receiver of the mth receive antenna as

$$r_m(t) = \sum_{n=1}^{N_T} \sum_{l=0}^{L-1} h_{mn}(l) s_n(t - lT_p) + w_m(t) \tag{3}$$

where $w_m(t)$ is the additive white Gaussian noise process with zero-mean and double-sided power spectral density of $N_0/2$. Here, only $L\left(L \le L_t\right)$ resolvable paths are assumed to be exploited by the receiver at each receive antenna for signal detection. By passing through a UWB pulse matched filter, the discrete-time received signal of the lth propagation path at the mth receive antenna denoted by $r_m(l)$, $l = 0,1,\cdots,L-1$, can be obtained. Then, the received signal vector, $\mathbf{r}(l) = \left[\, r_1(l)\ r_2(l)\ \cdots\ r_{N_R}(l) \,\right]^T$, at the matched filter output for the lth path can be described as

$$\mathbf{r}(l) = \sqrt{E_b}\ \mathbf{H}(l)\ \mathbf{b} + \mathbf{w}(l) \tag{4}$$

where $\mathbf{b} = \left[\, b_1\ b_2\ \cdots\ b_{N_T} \,\right]^T$ represents the information bit vector over N_T transmit antennas and $\mathbf{w}(l) = [w_1(l)\ w_2(l)\ \cdots\ w_{N_R}(l)]^T$ denotes the noise vector received on N_R receive antennas. For the lth delayed path, the discrete-time channel gains among all pairs of transmit receive antennas can be formed as an $N_R \times N_T$ matrix $\mathbf{H}(l) = [\mathbf{h}_1(l)\ \mathbf{h}_2(l)\ \cdots\ \mathbf{h}_{N_T}(l)]$ where the nth column vector is given by $\mathbf{h}_n(l) = [h_{1n}(l)\ h_{2n}(l)\ \cdots\ h_{N_R n}(l)]^T$. Note that we omit the bit index k because we focus on a particular bit of the transmitted data.

III. MIMO Detection Schemes

In this section, we consider three MIMO detection approaches for SM UWB MIMO systems employing 2PAM in UWB TDL indoor log-normal multipath fading channels with AWGN. We first introduce two previous SM MIMO detection architectures and then present an LR-based signal detection scheme including theoretical performance analysis.

A. ZF-MRC Detection Scheme [11]

The MIMO detection technique investigated in [11] employs a ZF filter to spatially demultiplex the multiplexed data streams from N_T transmit antennas on each multipath component and thus requires L ZF filters. A Rake receiver for MRC is then applied to combine the outputs of L ZF detectors. In this ZF-MRC scheme, the output signal vector, $\mathbf{y}(l) = [y_1(l)\ y_1(l)\ \cdots\ y_{N_R}(l)]^T$, of a ZF filter for the lth path of a particular bit is given by $\mathbf{y}(l) = \mathbf{H}(l)^\dagger\, \mathbf{r}(l)$ where $\mathbf{H}(l)^\dagger = \left(\mathbf{H}(l)^H \mathbf{H}(l)\right)^{-1} \mathbf{H}(l)^H$ represents the Moore-Penrose pseudo-inverse of the channel matrix $\mathbf{H}(l)$ for the lth path. Here $(\cdot)^\dagger$ and $(\cdot)^H$ denote the pseudo-inverse and conjugate transpose, respectively. The sufficient statistic of the MRC output for a particular bit of the nth transmitted data stream is expressed as

$$d_n = \sum_{l=0}^{L-1} \alpha_n^2(l)\, y_n(l) \tag{5}$$

where

$$\alpha_n^2(l) = \frac{1}{\left[\left(\mathbf{H}(l)^H \mathbf{H}(l)\right)^{-1}\right]_{nn}} \tag{6}$$

Here, $[\cdot]_{nn}$ is the nth diagonal element of main diagonal matrix. Remember that the (N_R, N_T, L) SM UWB MIMO system employing the ZF-MRC detection scheme achieves the diversity order of $D_{ZF-MRC} = L(N_R - N_T + 1)$.

B. MRC-ZF Detection Scheme [12]

In order to enhance the diversity order of the (N_R, N_T, L) SM UWB MIMO system, a different detection structure adopting 2-dimensional Rake combining in time and space domain (which is an MRC-ZF receiver) has been proposed in [12]. The Rake MRC operation is first performed to exploit both spatial diversity and multipath diversity, and then a single ZF detector is applied to spatially separate the data streams transmitted from N_T transmit antennas. That is, after spatial-temporal combining all multipath components, the Rake MRC output signal vector is written as

$$\mathbf{u} = \sum_{l=0}^{L-1} \mathbf{H}(l)^H \mathbf{r}(l) \tag{7}$$

Let the $LN_R \times N_T$ channel matrix including L multipath components be defined as

$$\mathbf{H} = \left[\, \mathbf{H}(0)^T \; \mathbf{H}(1)^T \cdots \mathbf{H}(L-1)^T \,\right]^T \tag{8}$$

Then the decision variable of the signal vector zero-forced with the ZF filter matrix $\mathbf{G}_{MRC-ZF} = \left(\mathbf{H}^H \mathbf{H}\right)^{\dagger}$ can be given as

$$\mathbf{v} = \mathbf{G}_{MRC-ZF}\, \mathbf{u} = \sqrt{E_b}\; \mathbf{b} + \left(\mathbf{H}^H \mathbf{H}\right)^{\dagger} \sum_{l=0}^{L-1} \mathbf{H}(l)^H \mathbf{w}(l) \tag{9}$$

When the MRC-ZF receiver is used, the achievable diversity order is evaluated as $D_{MRC-ZF} = L\,N_R - N_T + 1$.

C. LR-Based 2Rake-ZF Detection Scheme

Although the diversity order of the MRC-ZF is larger than that of the ZF-MRC in the presence of resolvable multipath components, it can't achieve the full diversity gain originating from the multipath diversity and receive diversity, which is equal to the product of L and N_R. Therefore, we present an LR-assisted 2Rake-ZF detection scheme, as shown in Fig. 1, for obtaining the maximum diversity gain. It carries out spatial combining and multipath diversity combining (i.e., 2-dimensional Rake combining in space and time domain) utilizing the LR matrix and then LR-based ZF detection is performed. This detection method is named as an LR-2Rake-ZF detector. Considering all multipath components, the system model in (4) can be represented as

$$\mathbf{r} = \sqrt{E_b}\;\mathbf{H}\,\mathbf{b} + \mathbf{w} = \sqrt{E_b} \sum_{n=1}^{N_T} \mathbf{h}_n b_n + \mathbf{w} \tag{10}$$

where $\mathbf{r} = [\,\mathbf{r}(0)^T \; \mathbf{r}(1)^T \cdots \mathbf{r}(L-1)^T\,]^T$ and $\mathbf{w} = [\,\mathbf{w}(0)^T \; \mathbf{w}(1)^T \cdots \mathbf{w}(L-1)^T\,]^T$. Here $\mathbf{h}_n$ is the nth column vector of $\mathbf{H}$ given as (8) and defined as

$$\mathbf{h}_n = \left[\, \mathbf{h}_n(0)^T \; \mathbf{h}_n(1)^T \cdots \mathbf{h}_n(L-1)^T \,\right]^T \tag{11}$$

The combinations $\sum_{n=1}^{N_T} \mathbf{h}_n b_n$ in (10) can be viewed as a real-valued lattice with basis vectors $\{\mathbf{h}_1, \mathbf{h}_2, \cdots, \mathbf{h}_{N_T}\}$. An LR operation is a process to determine a new basis for the given lattice, which consists of nearly orthogonal and relatively short vectors. In this work, the LR is performed by an Lenstra-Lenstra-Lovász (LLL) algorithm [15], [19], which is the most common LR technique. The received signal vector of (10) can rewritten in the LR domain as

$$\mathbf{r} = \sqrt{E_b}\;\mathbf{H}\mathbf{b} + \mathbf{w} = \sqrt{E_b}\;\tilde{\mathbf{H}}\mathbf{z} + \mathbf{w} \tag{12}$$

where $\tilde{\mathbf{H}} = \mathbf{H}\mathbf{T}$ and $\mathbf{z} = \mathbf{T}^{-1}\mathbf{b}$. Here $\mathbf{T}$ is an integer unimodular transformation matrix and $\tilde{\mathbf{H}}$ is a lattice basis reduced matrix whose column vectors are nearly orthogonal. Then the received signal vector for the lth path in the LR domain is given by

$$\mathbf{r}(l) = \sqrt{E_b}\;\mathbf{H}(l)\;\mathbf{b} + \mathbf{w}(l) = \sqrt{E_b}\;\tilde{\mathbf{H}}(l)\;\mathbf{z} + \mathbf{w}(l) \tag{13}$$

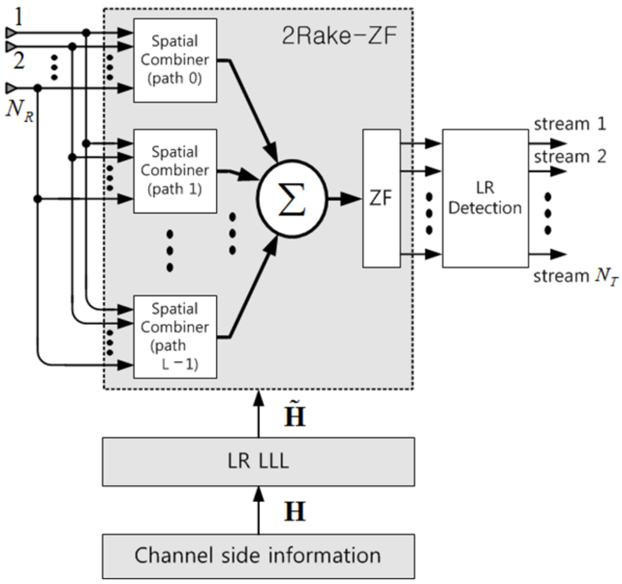

Fig. 1. LR-based 2Rake-ZF scheme.

Let the $LN_R \times N_T$ LR new channel matrix be defined by $\tilde{\mathbf{H}}\left(= [\,\tilde{\mathbf{H}}(0)^T \; \tilde{\mathbf{H}}(1)^T \cdots \tilde{\mathbf{H}}(L-1)^T\,]^T\right)$, which is a reduced version of $\mathbf{H}$ generated by the LLL algorithm. In the LR-2Rake-ZF receiver, the received signal vector of the lth path is spatially combined by the conjugate transpose of the subchannel matrix $\tilde{\mathbf{H}}(l)\left(= \mathbf{H}(l)\mathbf{T}\right)$ of $\tilde{\mathbf{H}}$. With $\tilde{\mathbf{H}}(l)$, the output signal vector of a spatial combiner corresponding to the lth path is given as

$$\mathbf{q}(l) = \tilde{\mathbf{H}}(l)^H \mathbf{r}(l) \tag{14}$$

For temporal combining to collect multipath diversity, the 2Rake output is obtained as

$$\tilde{\mathbf{u}} = \sum_{l=0}^{L-1} \mathbf{q}(l) \tag{15}$$

To spatially separate the transmitted signals from all N_T transmit antennas in the LR-based 2Rake architecture, a single LR-assisted ZF detector is applied to the 2Rake output signal. Here, the LR-based 2Rake-ZF filter employs the pseudo-inverse of a spatially and temporally combined version of the LR channel matrix, which is defined as

$$\mathbf{G}_{LR-2Rake-ZF} = \left(\sum_{l=0}^{L-1}\tilde{\mathbf{H}}(l)^H\tilde{\mathbf{H}}(l)\right)^{\dagger} = \left(\tilde{\mathbf{H}}^H\tilde{\mathbf{H}}\right)^{\dagger} \quad (16)$$

Then the output signal vector of the LR-aided 2Rake-ZF detector can be written as

$$\begin{aligned}\tilde{\mathbf{v}} &= \mathbf{G}_{LR-2Rake-ZF}\tilde{\mathbf{u}} \\ &= \mathbf{z} + \left(\tilde{\mathbf{H}}^H\tilde{\mathbf{H}}\right)^{\dagger}\sum_{l=0}^{L-1}\tilde{\mathbf{H}}(l)^H\mathbf{w}(l)\end{aligned} \quad (17)$$

In this work, the average energy per bit is assumed to be a unity. The estimate of $\mathbf{z}$ can be obtained from $\tilde{\mathbf{v}}$ in (17) as

$$\hat{\mathbf{z}} = 2\lceil 0.5(\tilde{\mathbf{v}} - \mathbf{T}^{-1}\mathbf{1}_{N_T})\rfloor + \mathbf{T}^{-1}\mathbf{1}_{N_T} \quad (18)$$

where $\lceil\bullet\rfloor$ dictates the rounding operation. Finally, the estimated signal vector $\hat{\mathbf{z}}$ in the LR domain is converted into the original signal constellation set by computing $\mathbf{T}\hat{\mathbf{z}}$ to recover $\mathbf{b}$.

From the output signal vector (17) of the LR-based 2Rake-ZF detector (which can be viewed as a decision variable for $\mathbf{z}$ prior to quantization), the instantaneous noise power on the nth data stream is easily obtained as

$$\begin{aligned}&\left[E\left\{\left(\tilde{\tilde{\mathbf{H}}}^{\dagger}\sum_{l=0}^{L-1}\tilde{\mathbf{H}}(l)^H\mathbf{w}(l)\right)\left(\tilde{\tilde{\mathbf{H}}}^{\dagger}\sum_{l=0}^{L-1}\tilde{\mathbf{H}}(l)^H\mathbf{w}(l)\right)^H\right\}\right]_{nn} \\ &= \left(\frac{N_0}{2}\right)\left[\tilde{\tilde{\mathbf{H}}}^{-1}\right]_{nn}\end{aligned} \quad (19)$$

where $\tilde{\tilde{\mathbf{H}}} = \tilde{\mathbf{H}}^H\tilde{\mathbf{H}}$ is assumed to be a full rank. Thus the corresponding post-processing SNR can be expressed as [11]

$$\rho_{n,LR-2Rake-ZF} = \frac{2}{N_0\left[\tilde{\tilde{\mathbf{H}}}\right]_{nn}^{-1}} = \frac{2}{N_0}\tilde{\mathbf{h}}_n^H\tilde{\mathbf{F}}\tilde{\mathbf{h}}_n \quad (20)$$

where $\tilde{\mathbf{h}}_n$ is the nth column vector of $\tilde{\mathbf{H}}$, which is defined as

$$\tilde{\mathbf{h}}_n = \left[\tilde{\mathbf{h}}_n(0)^T \ \tilde{\mathbf{h}}_n(1)^T \ \cdots \ \tilde{\mathbf{h}}_n(L-1)^T\right]^T \quad (21)$$

and $\tilde{\mathbf{F}}$ is an $LN_R \times LN_R$ non-negative Hermitian matrix constructed from $\tilde{\mathbf{h}}_1, \cdots, \tilde{\mathbf{h}}_{n-1}, \tilde{\mathbf{h}}_{n+1}, \cdots, \tilde{\mathbf{h}}_{N_T}$. That is, $\tilde{\mathbf{F}} = \tilde{\mathbf{H}}_n\tilde{\mathbf{H}}_n^H / \det\left[\tilde{\mathbf{H}}_n^H\tilde{\mathbf{H}}_n\right]$ where $\tilde{\mathbf{H}}_n$ denotes the matrix obtained from excluding the column vector $\tilde{\mathbf{h}}_n$ from the matrix $\tilde{\mathbf{H}}$.

To simplify the analysis of diversity gain in this work, we assume that the LR matrix $\tilde{\mathbf{H}}$ consists of perfectly orthogonal column vectors. In this case, $\tilde{\mathbf{h}}_n$ and its projection on the subspace of $\tilde{\mathbf{F}}$ are orthogonal. Then the SNR expression of (20) can be simplified as

$$\rho_{n,LR-2Rake-ZF} = \frac{2}{N_0}\left\|\tilde{\mathbf{h}}_n\right\|^2 = \frac{2}{N_0}\sum_{i=1}^{LN_R}\left|\tilde{h}_n^{(i)}\right|^2 \quad (22)$$

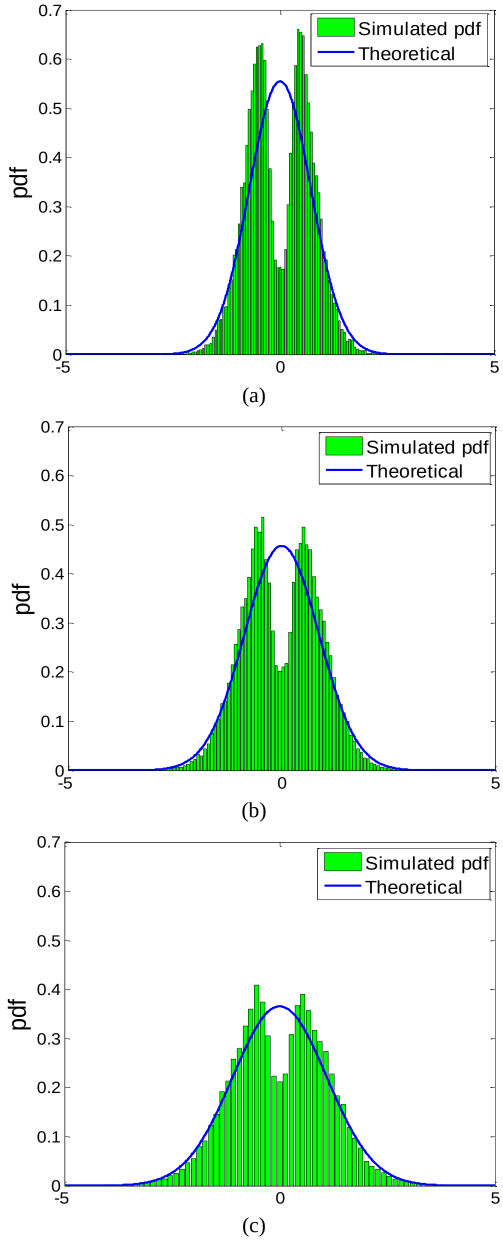

Fig. 2. Approximated pdf of $\tilde{h}_i^{(1)}$ for the (3,3,2) UWB system: (a) $\tilde{h}_1^{(1)}$, (b) $\tilde{h}_2^{(1)}$, and (c) $h_3^{(1)}$.

where $\tilde{h}_n^{(i)}$ is the ith element of the vector $\tilde{\mathbf{h}}_n$. As an additional simplification, $\tilde{h}_n^{(i)}$ will be intentionally fitted into an approximated Gaussian random variable with zero-mean and variance $\sigma_n^{(i)^2}$ for the purpose of theoretical analysis in respect of diversity gain and BER performance. Thus it is shown in Fig. 2 that the simulated histograms of $\tilde{h}_1^{(1)}$, $\tilde{h}_2^{(1)}$, and $\tilde{h}_3^{(1)}$ for the $(N_T, N_R, L) = (3,3,2)$ SM UWB MIMO system are forcibly approximated as pdfs of Gaussian distribution with a variance of $\sigma_1^{(1)^2} = 0.5170$, $\sigma_2^{(1)^2} = 0.7618$, and

$\sigma_3^{(1)^2} = 1.1912$, respectively. The value of each $\sigma_n^{(i)^2}$ is affected by the LR operation trying to yield reduced bases with shorter basis vectors and thus depends on the values of L, N_R, N_T, and δ, which are parameters selected in the LLL algorithm [15]. It is observed that the average value of three variances, $E\left[\sigma_n^{(1)^2}\right] =$ 0.8233, is less than unit-variance, which has been assumed as the variance of the approximated Gaussian random variable in [11] and [12] for the case without LR. Here the standard deviation of log-normal fading amplitude is assumed to be 5-dB and the LLL algorithm with $\delta = 1$ is used.

With an assumption that $\tilde{x}_n^{(i)}$ is a Gaussian random variable with zero-mean and unit-variance, $\tilde{h}_n^{(i)}$ can be expressed as $\tilde{h}_n^{(i)} = E\left[\sigma_n^{(i)}\right] \tilde{x}_n^{(i)} = \sqrt{c_\delta}\, \tilde{x}_n^{(i)}$ where c_δ is the average variance of the approximated Gaussian pdfs. Thus, $E\left[\tilde{\mathbf{h}}_n \tilde{\mathbf{h}}_n^H\right] = diag\left\{c_\delta, c_\delta, \cdots, c_\delta\right\} = c_\delta \mathbf{I}_{LN_R}$. Then the SNR expression of (22) can be described as

$$\rho_{n,LR-2Rake-ZF} = \frac{2}{N_0} c_\delta \sum_{i=1}^{LN_R} \left| \tilde{x}_n^{(i)} \right|^2 = \frac{2}{N_0} c_\delta \rho_{n,0} \qquad (23)$$

Hence, $\rho_0 = \sum_{i=1}^{LN_R} \left| \tilde{x}_n^{(i)} \right|^2$ can be assumed to be central Chi-square distributed with $D_{LR-2Rake-ZF} = LN_R$ degrees of freedom and its pdf is given by

$$f_{\rho_0}(t) = \frac{t^{0.5D_{LR-2Rake-ZF}-1} e^{-0.5t}}{2^{0.5D_{LR-2Rake-ZF}}\, \Gamma\left(0.5D_{LR-2Rake-ZF}\right)} \qquad (24)$$

where $\Gamma(\cdot)$ is the gamma function. By averaging the conditional BER expression given by

$$P_{b\left|\rho_{n,LR-2Rake-ZF}\right.}(t) = 0.5erfc\left(\sqrt{\frac{c_\delta}{N_0} t}\right) = Q\left(\sqrt{\frac{2c_\delta}{N_0} t}\right) \qquad (25)$$

over $f_{\rho_0}(t)$, the average BER of the LR-2Rake-ZF detection scheme in a log-normal fading channel can be computed as

$$P_{b,LR-2Rake-ZF} = \int_0^\infty P_{b\left|\rho_{n,LR-2Rake-ZF}\right.}(t)\, f_{\rho_0}(t)\, dt \qquad (26)$$

It is pointed out that in order to compute the theoretical BER performances from the expression (26), the value of c_δ should be required. In this work, the variances, $\sigma_n^{(i)^2}$, $n = 1, 2, \cdots, N_T$, obtained through simulations approximating as Gaussian pdf as in Fig. 2 are averaged out to get the value of c_δ. Note that the variance of the approximated Gaussian pdf could be varying according to the size of the $LN_R \times N_T$ channel matrix $\tilde{\mathbf{H}}$ and the value of δ in the LLL algorithm. Eventually it could affect the output SNR value of (23). As the value of δ increases up to 1 from 0.25, the variance c_δ of the approximated Gaussian pdf gets smaller. Although the perfect orthogonality is assumed in the process of developing an approximated analytic BER expression, the variance c_δ is calculated using the parameter $\delta = 1$ in the LLL algorithm and then the computed variance c_δ is applied to the SNR expression to obtain the theoretical BER results.

IV. Computational Complexity Comparison

In order to simply compare the computational complexities of the ZF-MRC, MRC-ZF, and LR-2Rake-ZF, we take account of only the multiplicative operation in the manipulations of a matrix by a matrix and a matrix by a vector (other computational operation is ignored) [12]. The complexities of the ZF-MRC and MRC-ZF presented in [12] are shown in Table 1. Since the LR-2Rake-ZF detector can be regarded as an extension of the MRC-ZF in LR domain, it requires an additional computational effort due to the LLL algorithm, which is denoted by $f_{LLL}(L, N_R, N_T)$. In this wok, it is evaluated as $f_{LLL}(L, N_T) = O\left(L^3 N_T^3 \log\left(LN_T\right)\right)$ for the case of $N_R = N_T$, which is given as an upper bound of the average complexity of an effective LLL algorithm [20]. Note that the LR-2Rake-ZF detector presents full diversity with acceptable complexity for small-medium values of L and N_T considered in the simulations. Table I summarizes the complexity comparison for UWB MIMO detection schemes covered in this work.

TABLE I. Complexity Comparison of UWB MIMO Detectors

	Complexity
ZF-MRC	$O\left(LN_T^3\right) + 2LN_R N_T^2 + LN_R N_T$
MRC-ZF	$O\left(N_T^3\right) + 2N_T^3 + LN_R N_T^2 + N_R N_T$
LR-2Rake-ZF	$O\left(N_T^3\right) + 2N_T^3 + LN_R N_T^2 + N_R N_T + f_{LLL}(L, N_R, N_T)$

V. Simulation Results

In all simulations, for the (N_T, N_R, L) SM UWB MIMO systems, we define the SNR per bit in decibel as $SNR = 2E_b/N_0\,(dB) + 10\log_{10} D$ where D is the diversity order of each UWB MIMO detector. Here $D = D_{ZF-MRC} = L\left(N_R - N_T + 1\right)$, $D = D_{MRC-ZF} = LN_R - N_T + 1$, and $D = D_{LR-2Rake-ZF} = LN_R$, respectively, are used for ZF-MRC, MRC-ZF, and LR-2Rake-ZF detectors. Recall that this work assumes $E_b = 1$. The expression of log-normal fading amplitude can be described as $\beta_{mn}(l) = e^{\varphi_{mn}(l)}$ [11], where $\varphi_{mn}(l)$ is Gaussian-distributed with $N\left(\mu_{\varphi_{mn}(l)}, \sigma_\varphi^2\right)$. Here a variance σ_φ^2 is assumed to be independent of indexes *l*, *m*, and *n*. We use 5-dB as a standard deviation of $20\log_{10}\beta_{mn}(l)$ $\left(= \varphi_{mn}(l)\left(20\log_{10} e\right)\right)$. Moreover, to meet $E\left[\beta_{mn}(l)^2\right] = e^{-\gamma l}$, which stands for the *l*th path's average power, it is required that $\mu_{\varphi_{mn}(l)} = -\sigma_\varphi^2 - \gamma l/2$ with $\sigma_\varphi = 5/\left(20\log_{10} e\right)$. In this work, it is assumed that the average power of the 0th multipath component is a unity and the power decay factor of $\gamma = 0$ is selected. The channel-state information of all L resolvable paths is assumed to be known only at the receivers. In all plots, analytic and simulated BER curves of the SM UWB (N_T, N_R, L) MIMO systems with three different detection schemes of ZF-MRC, MRC-ZF, and LR-2Rake-ZF are shown with lines and markers, respectively. All figures plot the BER performance as a function of E_b/N_0 in decibels. In the LR LLL algorithm, the analytic BER results are obtained with the parameter $\delta = 1$ while the simulated BER performances adopt $\delta = 0.5$ for signal detection.

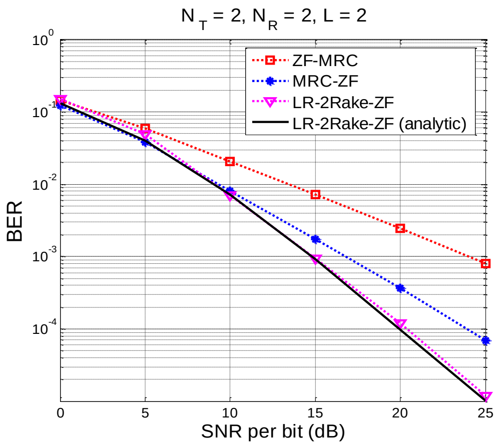

Fig. 3. BER comparison of SM UWB MIMO detection schemes in the (2, 2, 2) system, and $c_\delta = 0.8561$ is used for analytical BER.

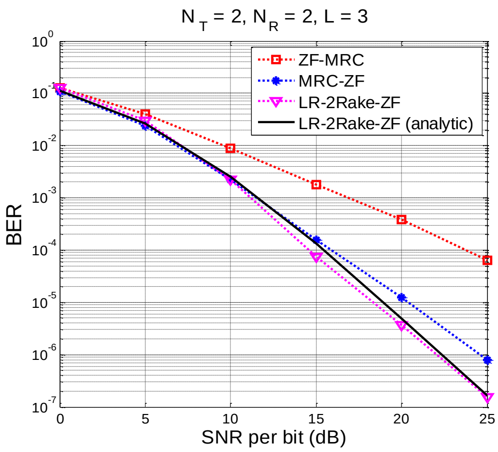

Fig. 4. BER comparison of SM UWB MIMO detection schemes in the (2, 2, 3) system, and $c_\delta = 0.9201$ is used for analytical BER.

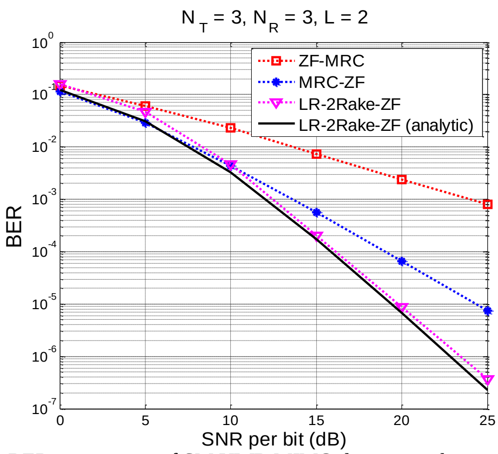

Fig. 5. BER comparison of SM UWB MIMO detection schemes in the (3, 3, 2) system, and $c_\delta = 0.8319$ is used for analytical BER.

Fig. 3 and Fig. 4, respectively, show the analytical and simulated BER results of ZF-MRC, MRC-ZF, and LR-2Rake-ZF receivers for the $(2,2,2)$ and $(2,2,3)$ SM UWB MIMO systems. In Fig. 5, Fig. 6, and Fig. 7, the $(3,3,2)$, $(3,3,3)$, and $(3,3,4)$ SM UWB MIMO systems are considered.

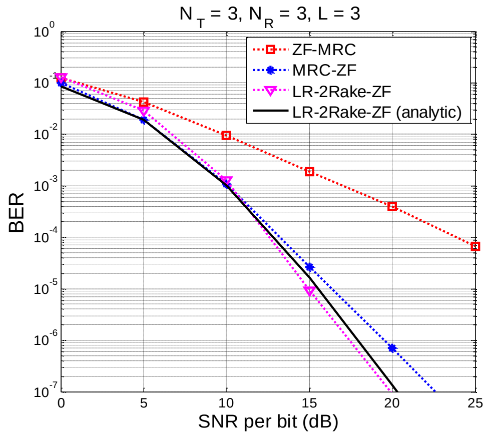

Fig. 6. BER comparison of SM UWB MIMO detection schemes in the (3, 3, 3) system, and $c_\delta = 0.9175$ is used for analytical BER.

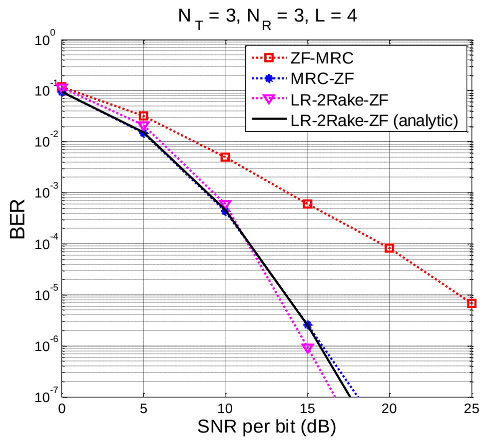

Fig. 7. BER comparison of SM UWB MIMO detection schemes in the (3, 3, 4) system, and $c_\delta = 0.9538$ is used for analytical BER.

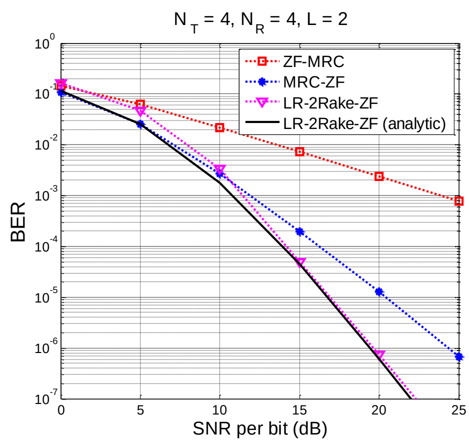

Fig. 8. BER comparison of SM UWB MIMO detection schemes in the (4, 4, 2) system, and $c_\delta = 0.8308$ is used for analytical BER.

Fig. 8 and Fig. 9 deal with the $(4,4,2)$ and $(3,4,2)$ SM UWB MIMO systems. It is found that the LR-2Rake-ZF receiver outperforms the MRC-ZF in the ranges of medium to high SNR values in addition to the ZF-MRC. It can achieve the full diversity order of LN_R while the diversity order of MRC-ZF is $LN_R - N_T + 1$. The title of each figure includes the variance c_δ computed as mentioned in Section III to obtain the analytical BER value. It is observed that the analytical BERs match relatively well the simulated ones for the given system parameters. Although the analytical BER results are slightly different from the simulated ones depending on the simulation conditions, the diversity order of the one is similar to the other because their slopes are almost identical. It is observed that as the product of multipath components and the number of receive antennas increases, the BER results of the LR-2Rake-ZF detector are closer to that of the MRC-ZF. In other words, when the value of LN_R is much larger than the number of transmit antennas, the diversity order of the MRC-ZF approaches to the maximum diversity order of LN_R. It is also seen that the LR-2Rake-ZF detector works better as the number of multiple paths and/or the number of receive antennas increase.

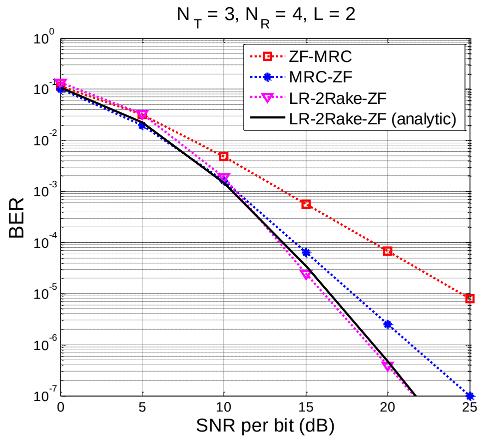

Fig. 9. BER comparison of SM UWB MIMO detection schemes in the (3, 4, 2) system, and $c_\delta = 0.8921$ is used for analytical BER.

VI. Conclusion

An LR-assisted detection scheme is proposed for SM UWB MIMO systems in log-normal multipath fading channels. An LR technique is shown to provide great BER performance improvements of ZF-based linear receivers in UWB systems, but require the extra computations of the reduced matrix by using an LLL algorithm. It is analyzed that the proposed LR-based detector called LR-2Rake-ZF achieves the maximum diversity gain of LN_R, which is larger than the diversity gain $L(N_R - N_T + 1)$ of the ZF-MRC and the diversity gain $LN_R - N_T + 1$ of the MRC-ZF. Simulations are conducted to confirm the analytical results.

Acknowledgment

This study was supported by research funds from Dong-A University.

References

[1] G. B. Giannakis and L. Yang, "Ultra-wideband communications: An idea whose time has come," *IEEE Signal Process. Mag*., vol. 21, no. 6, pp. 26–54, Nov. 2004.

[2] N. Rendevski and D. Cassioli, "60 GHz UWB rake receivers in a realistic scenario for wireless home entertainment," in *Proc. IEEE Int. Conf. Commun. (ICC)*, Jun. 2015, pp. 2744–2749.

[3] J. Zhang, P. V. Orlik, Z. Sahnoglu, A. F. Molisch, and P. Kinney, "UWB systems for wireless sensor networks," *Proc. IEEE*, vol. 97, no. 2, pp. 313-331, Feb. 2009.

[4] A. Paulraj, D. Gore, R. Nabar, and H. Bolcskei, "An overview of MIMO communications-A key to gigabit wireless," *Proc. IEEE*, vol. 92, no. 2, pp. 198-218, Feb. 2004.

[5] T. Kaiser, F. Zheng, and E. Dimitrov, "An overview of ultra-wide-band systems with MIMO," *Proc. IEEE*, vol. 97, no. 2, pp. 285-312, Feb. 2009.

[6] V. P. Tran and A. Sibille, "Spatial multiplexing in UWB MIMO communications," *Electronics Letters*, vol. 42, no. 16, pp. 931-932, Aug. 2006.

[7] T. Wang, T. Lv, H. Gao, and Y. Lu, "BER analysis of decision-feedback multiple-symbol detection in noncoherent MIMO ultrawideband systems," *IEEE Trans. Veh. Techol*., vol. 62, no. 9, pp. 4684-4690, Nov. 2013.

[8] R. D. Jalan, D. K. Rout, and S. Das, "Performance enhancement of MIMO/UWB based wireless body area network," in *Proc. IEEE Global Conf. Commun. Techol. (GCCT)*, 2015, pp. 604–609.

[9] S. Sharma, V. Bhatia, and A. Gupta, "Noncoherent IR-UWB receiver using massive antenna arrays for wireless sensor networks," *IEEE Sensors Lett*., vol. 2, no. 1, pp. 1–4, Mar. 2018.

[10] S. Sharma, A. Gupta, and V. Bhatia, "IR-UWB sensor network using massive MIMO decision fusion design and performance analysis," *IEEE Sensors Journal*, vol. 18, no. 15, pp. 6290–6302, Aug. 2018.

[11] H. Liu, R. C. Qiu, and Z. Tian, "Error performance of pulse-based ultra-wideband MIMO systems over indoor wireless channels," *IEEE Trans. Wireless Commun*., vol. 4, no. 6, pp. 2939-2944, Nov. 2005.

[12] J. An and S. Kim, "Spatial-temporal combining-based ZF detection in ultra-wideband communications," *IEICE Trans. Fundamentals*, vol. E92-A, no. 7, pp. 1727-1730, Jul. 2009.

[13] A. H. Mehana and A. Nosratinia, "Performance of linear receivers in frequency-selective MIMO channels," *IEEE Trans. Wireless Commun*., vol. 12, no. 6, pp. 2697-2705, Jun. 2013.

[14] M. Niroomand and M. Derakhtian, "A low complexity diversity achieving decoder based on a two-stage lattice reduction in frequency-selective MIMO channels," *IEEE Trans. Wireless Commun*., vol. 16, no. 4, pp. 2465-2477, Apr. 2017.

[15] D. Wübben, D. Seethaler, J. Jaldén, and G. Matz, "Lattice reduction: A survey with applications in wireless communications," *IEEE Trans. Signal Process. Mag*., vol. 28, no. 3, pp. 70-91, May 2011.

[16] Q. Huang and A. Burr, "Low complexity coefficient selection algorithms for compute-and-forward," *IEEE Access*, vol. 5, pp. 19182-19193, Oct. 2017.

[17] D. Cassioli, M. Z. Win, and A. F. Molisch, "The ultra-wide bandwidth indoor channel: From statistical model to simulations," *IEEE J. Sel. Areas Commun*., vol. 20, no. 6, pp. 1247-1257, Aug. 2002.

[18] J. Karedal, S. Wyne, P. Almers, F. Tufvesson, and A. F. Molisch, "Statistical analysis of the UWB channel in an industrial environment," in *Proc. IEEE VTC*, Los Angeles, CA, Sep. 2004, pp. 81-85.

[19] X. Ma and W. Zhang, "Performance analysis for MIMO systems with lattice-reduction aided linear equalization," *IEEE Trans. Commun*., vol. 56, no. 2, pp. 309-318, Feb. 2008.

[20] C. Ling and N. Howgrave-Graham, "Effective LLL reduction for lattice decoding," presented at IEEE Int. Symp. Inform. Theory, Nice, France, Jun. 2007.

Youngbeom Kim has received his B.S. degree in electronics engineering from Dong-A University, Busan, Korea in 2011. Currently, he is in the final semester of Master and Ph.D. integrated program in department of electronics engineering at Dong-A University. He is interested in 5G, MIMO technology, UWB communications, and signal detection.

Sangchoon Kim was born in Jeju, Korea, in 1965. He received the B.S. degree from Yonsei University, Seoul, Korea, in 1991 and the M.E. and Ph.D. degrees from the University of Florida, Gainesville, FL, USA, in 1995 and 1999, respectively, all in electrical and computer engineering. From 2000 to 2005, he has been a Senior Research Engineer in LG Corporate Institute of Technology, Seoul, Korea, and a Chief Research Engineer with the LG Electronics, Anyang, Korea, working on a range of research projects in the field of wireless/mobile communications. Since 2005, he has joined in Dong-A University, Busan, Korea and currently is a full professor with Department of Electronics Engineering, Dong-A University, Busan, Korea. His research interests have covered a range of areas in wireless/mobile communications, signal processing, and antenna design.